Entangled photon apparatus for the undergraduate laboratory

Dietrich Dehlinger and M. W. Mitchell[a)]
Physics Department, Reed College, 3203 SE Woodstock Boulevard, Portland, Oregon 97202

(Received 3 December 2001; accepted 13 June 2002)

We present detailed instructions for constructing and operating an apparatus to produce and detect polarization-entangled photons. The source operates by type I spontaneous parametric downconversion in a two-crystal geometry. Photons are detected in coincidence by single-photon counting modules and show strong angular and polarization correlations. We observe more than 100 entangled photon pairs per second. A test of a Bell inequality can be performed in an afternoon.

[DOI: 10.1119/1.1498859]

I. INTRODUCTION

The entanglement of particles is ubiquitous in quantum mechanical systems and is arguably the aspect of quantum theory most at odds with classical intuitions. Einstein, Podolsky, and Rosen first drew attention to the possibility of nonlocal effects involving entangled particles.[1] In the mid-sixties it was realized that the nonlocality of nature was a testable hypothesis and subsequent experiments confirmed the quantum predictions.[2] More recently, much effort has gone into exploiting the odd nature of entangled particles. Applications include secure cryptography, transmission of two bits of information with a single photon, and ''teleportation'' of a quantum state (by erasing the state of a system and then re-creating the state in a distant system).[3–9] Perhaps the most exciting possible application is in computing. A quantum computer that used entangled particles as data registers would be capable of performing calculations faster than any classical computer.[10–13]

Here we describe how to produce and detect entangled photons using equipment and techniques suitable for an undergraduate laboratory. This is possible due to recent advances in diode laser technology and new techniques for generation of photon pairs.[14,15] The total cost for the apparatus is approximately 15 000 USD.

II. OVERVIEW

In the process of spontaneous parametric downconversion a single pump photon spontaneously splits into ''signal'' and ''idler'' photons inside a nonlinear crystal.[16,17] Because the two downconverted photons come from a single parent photon, they have definite combined properties: their total energy and momentum (inside the crystal) must agree with the parent energy and momentum. They are also produced at very nearly the same time. The individual photons' properties are free to vary, however, and spontaneous parametric downconversion produces a spectrum of both signal and idler wavelengths centered around twice the parent photon wavelength. To satisfy phase matching requirements, which reflect the dispersion and birefringence of the crystal, these different wavelengths emerge in different directions and create a conical rainbow of emission as illustrated in Fig. 1.

By appropriate angular placement of the detectors, we select ''degenerate'' daughter photons, those that have the same wavelength $\lambda_S = \lambda_I = 2\lambda_{\text{pump}}$. Our crystals are cut for type I downconversion, in which the signal and idler photons have the same polarization, which is opposite to that of the pump photon.[18] A given crystal can only support type I downconversion of one pump polarization, the other polarization simply passes through the transparent crystal. Our source uses two identical crystals, with one rotated 90° from the other about the beam propagation direction, as shown in Fig. 2. In this arrangement each crystal can support downconversion of one pump polarization. A 45° polarized pump photon can downconvert in either crystal, producing a polarization-entangled pair of photons.[17]

Figure 3 shows a schematic of the experimental setup. A 5-mW, 405-nm, InGaN laser diode (Nichia Model NLHV500C) is the source of pump photons. The diode is driven at its specified operating current with a precision constant current source capable of supplying the 5-V operating voltage of the InGaN laser. The beam is focused with an aspheric lens mounted in a collimating tube, which is held in a vee-mount glued to a mirror mount. The beam focus is adjusted to produce a beam diameter of about 1 mm at 1 m from the laser.

The laser beam passes a BG12 colored glass filter, a beam aperture consisting of a sheet of aluminum with a small hole drilled in it, a glass linear polarizer on a rotating mount, a 0.5-mm-thick quartz plate mounted to rotate about the vertical (the crystal's fast axis), and a second beam aperture before reaching the nonlinear crystals. The apertures and filter act to remove unwanted light and the polarizer and quartz plate set the laser polarization.

The nonlinear crystals are two beta barium borate (BBO) crystals, 5 mm×5 mm×0.1 mm thick, cut with their crystal axes at 29° from the normal to the large face. The crystals are mounted face-to-face with one crystal rotated by 90° about the normal to the large face. The crystal holder is held in a mirror mount and aligned to be perpendicular to the laser beam direction. A beam stop blocks the laser beam after it passes alongside the detectors.

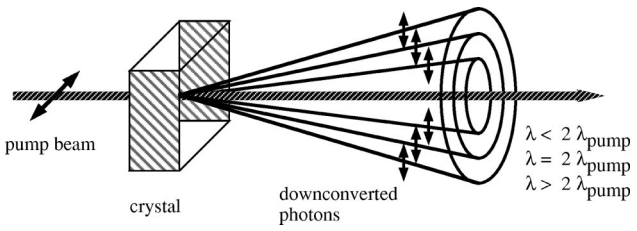

Fig. 1. Type I spontaneous parametric downconversion. Photons from a pump beam split into pairs of photons.

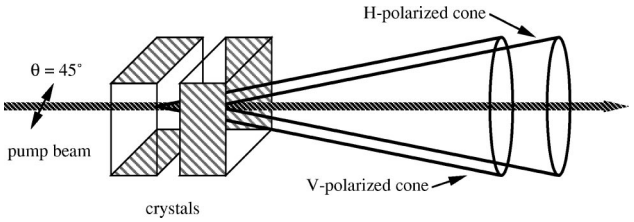

Fig. 2. Two-crystal downconversion source.

The downconverted photons produced in the BBO crystals travel about 1 m before passing an adjustable 1-in.-diam iris diaphragm, a plastic film near-infrared polarizer on a rotatable mount, a 1-in.-diam RG780 colored glass filter, and are focused by a 75-mm focal length lens onto the detector surface. The RG780 is a long-pass filter with a 50% transmission at 780 nm. For a coincidence detection event to occur, both signal and idler photons, which are roughly equally spaced in wavelength about 810 nm, must pass RG780 filters. Thus a wavelength band (in the signal photon) of about 780–840 nm can lead to coincidence detection.

The detectors (Perkin–Elmer Optoelectronics model SPCM-AQR-13) are silicon avalanche photodiodes run in Geiger mode, called single-photon counting modules (SPCMs).[19,20] To aid in focusing, each detector was mounted on standard optical mounting posts and a 30-mm ''cage'' assembly was attached to hold the lens and RG780 filter. These are described in Sec. III. The lens is held in an X–Y translator for fine adjustment of the lens position.

Along each detection path, the detector, lens, filter, polarizer, and iris are mounted on an aluminum rail which pivots about an optical post directly below the crystals. This arrangement allows adjustment of the angular position of the detectors without losing focus. Although we performed our experiments on an optical table, we note that this is probably unnecessary. Interferometric stability is not required, and the rails maintain the necessary alignment. We expect the experiment could be performed on an optical breadboard or other flat surface.

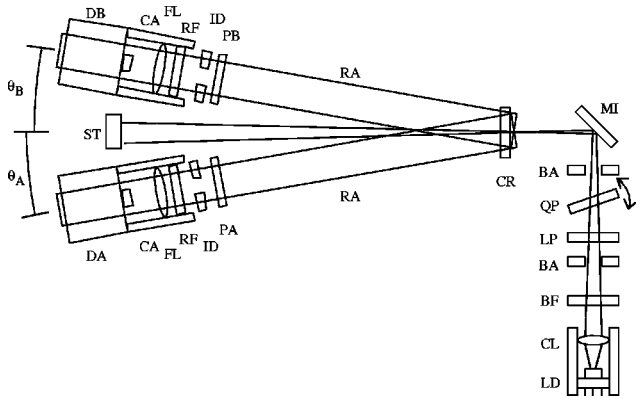

Fig. 3. Schematic of experimental setup, not to scale. Symbols: (LD) laser diode, (CL) collimating lens, (BF) blue filter, (BA) beam aperture, (LP) laser polarizer, (QP) quartz plate, (MI) mirror, (CR) downconversion crystals, (RA) rail, (PA) polarizer A, (PB) polarizer B, (ID) iris diaphragm, (RF) red filter, (FL) focusing lens, (CA) cage assembly, (DA) detector A, (DB) detector B, (ST) beam stop.

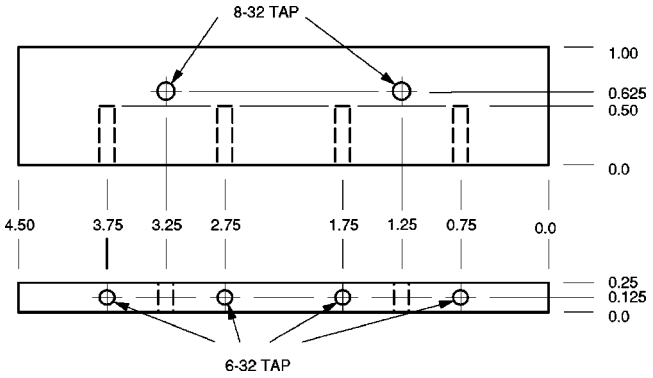

Fig. 4. Single-photon counting module (SPCM) base adapter plate. Units: inches, all tolerances are ±0.01 in. unless otherwise specified.

III. MECHANICS

The first version of the detection setup used independent table-mounted components to hold the filters and position the focusing lenses. This early setup was quick to assemble from common components such as translation stages and lens holders, but was difficult to align and required near-complete darkness. For greater ease of use we developed the mechanical system described below.

The SPCMs, as furnished by the manufacturer, do not directly interface to standard optical hardware. We built two simple adapter plates, shown in Figs. 4 and 5. The base adapter allows the detector to be mounted on standard optical posts, while the front adapter allows a cage assembly to be attached to the detector, as shown in Fig. 6. The cage assembly consists of four rods, each 4 in. long, held at the detector end by a 30-mm cage plate and at the other end by a 30-mm X–Y translator which holds the focusing lens and filter. The cage plate attaches to the front adapter by a threaded tube and a retaining ring. This same tube presses against a gasket of black closed-cell foam to make a light-tight seal. Other threaded tubes link the X–Y translator to the cage plate. This

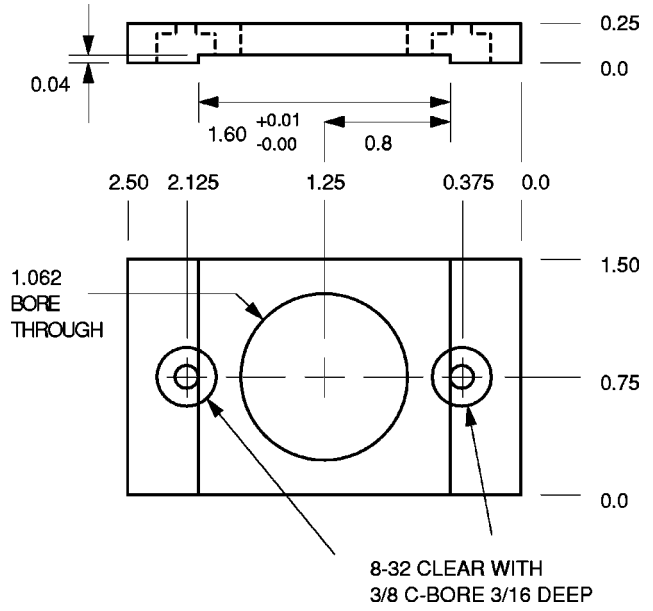

Fig. 5. SPCM front adapter plate. Units: inches, all tolerances are ±0.01 in. unless otherwise specified.

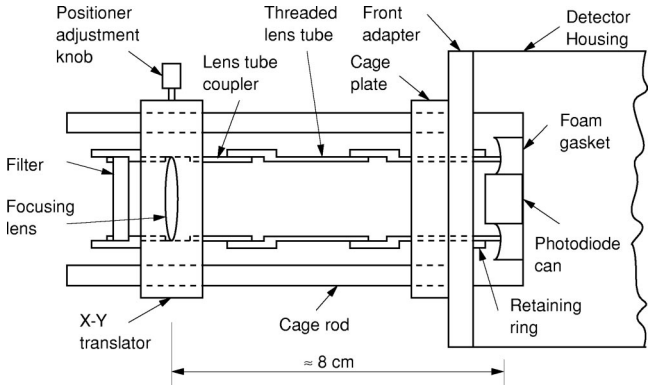

Fig. 6. Schematic of detector-mounted cage assembly, side view.

arrangement has two principal advantages. First, the path from filter to detector is entirely enclosed, greatly reducing sensitivity to stray light and protecting the detector from mechanical damage. Second, precise positioning of the focusing lens is easily accomplished by sliding the $X-Y$ translator along the rails and adjusting the $X-Y$ translation knobs. Because the lens sits about 1-m away from the crystals, the image of the crystals on the detector moves by about 75 μm for every 1 mm displacement of the lens. This is handy as the detector's active area is only 180 μm in diameter.

Each detector and cage assembly, as well as the associated iris and polarizer, sit upon a detector rail as shown in Fig. 3. We constructed our rails from $\frac{1}{2}$-in.-thick aluminum bars, as shown in Fig. 7. Four post holders are mounted directly to the rail to hold the detector, iris, and linear polarizer. A $\frac{1}{2}$-in.-diam hole at the opposite end from the detector fits over a standard (0.499-in.-diam) optical post which serves as a pivot for the rail. The second rail pivots about the same post, sitting upon the first rail. A $\frac{1}{2}$-in.-high spacer beneath the second rail on the detector end allows the rail to sit flat on the table.

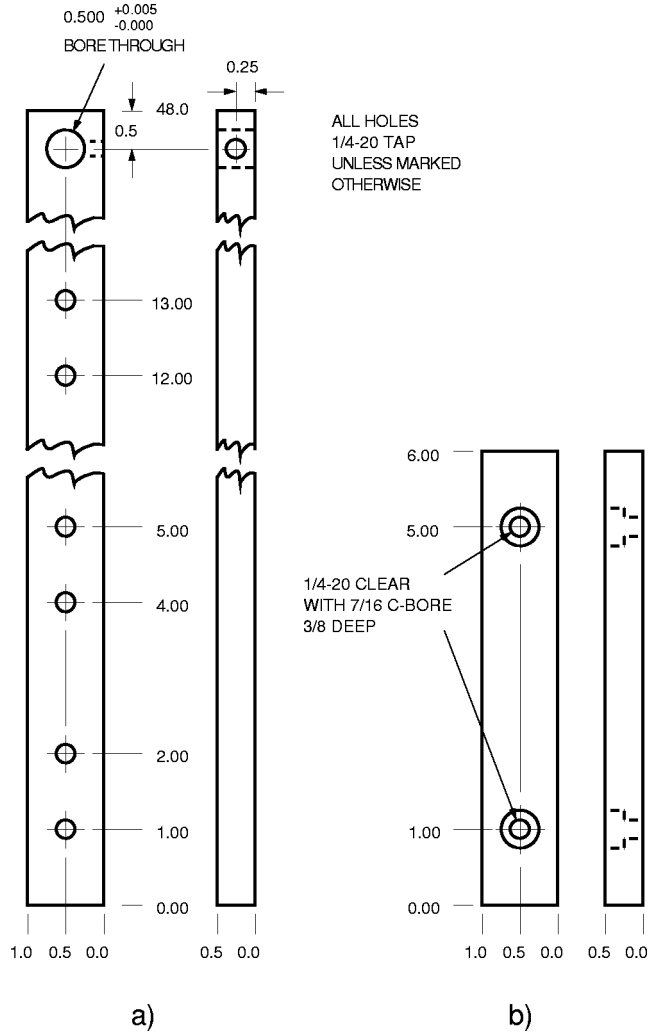

Fig. 7. Detector rail. (a) rail, (b) under-rail spacer. All parts are aluminum. Units: inches, all tolerances are ± 0.01 in. unless otherwise specified.

IV. ELECTRONICS

Detection of a photon by a SPCM produces a short (about 25-ns) TTL pulse. To identify photons from spontaneous parametric downconversion within the background of fluorescence photons, we record coincident detections. Our first coincidence detector used a NIM standard time-to-amplitude converter and a multichannel analyzer (MCA). This setup required converting the TTL pulses to NIM pulses and also required a computer to record data from the MCA. A simpler and far less expensive alternative is to build a coincidence circuit from fast logic chips. A schematic for such a circuit is shown in Fig. 8.

The circuit is built from two 74ACT74 dual D-type positive edge-triggered flip-flops, or four D-type flip-flops in all. Starting at the lower left of the diagram and working clockwise, the first flip-flop delays the B pulse by the time required to clock and reset, 6.5–19.5 ns by the manufacturer's specifications. The next flip-flop produces a stretched pulse at A OUT. The next performs the coincidence detection: If A IN is already high when the delayed B pulse arrives, a stretched pulse is produced at COINC OUT. The coincidence window is the duration of the A IN pulse. The final flip-flop stretches the B pulse. The inputs are 50 Ω terminated. The outputs pulses are all TTL compatible and about 250 ns long. Longer pulses can be produced by increasing the values of the capacitors. The output pulses are fed to the counter-timer inputs of a PC-based data acquisition board.

The coincidence circuit is simple to build, but as with any fast electronics, proper construction technique is necessary for good performance. It is helpful to have a fast oscilloscope when debugging this circuit.

V. ALIGNMENT

The apparatus is not difficult to align if done in the correct order. All optical elements should be set to the same height above the table. With the crystals, polarizers, and RG780 filters removed from the setup, the remaining rail-mounted components (detectors, lenses, and irises) can be aligned as follows. The detector is viewed from the position the crystals will occupy, through the open iris and lens. The detector's active area is a circular black spot at the center of a gold square. By aligning and focusing the lens, the detector's active area can be made to fill the field of view. The iris should be centered on this image.

Once this rough alignment is performed, the crystals, polarizers and RG780 filters can be put in place. The laser is aligned to pass through the crystals' center. The rails should be positioned on opposite sides of the laser beam, each about

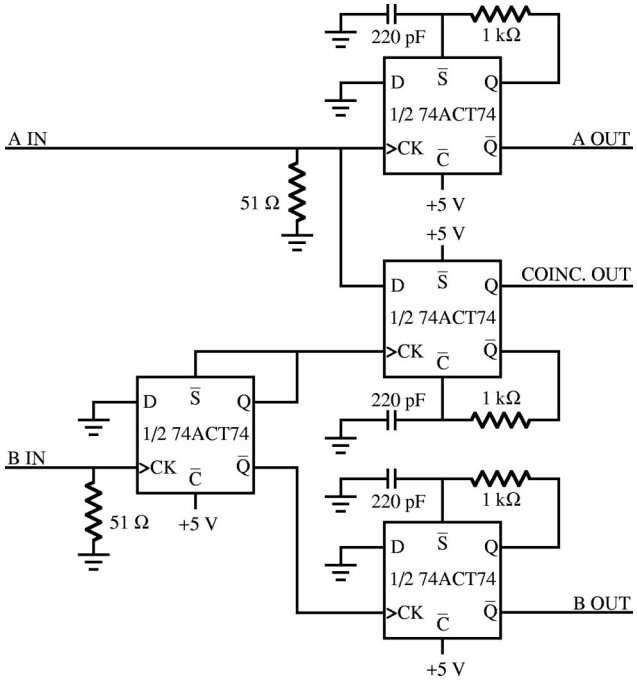

Fig. 8. Schematic of coincidence detection circuit. See the text for details.

three degrees away from the beam. With the room darkened, fine adjustments in lens position can be made to maximize the singles count rate at each detector. Finally, the angles of the rails should be adjusted to maximize the coincidence detection rate. Following this procedure we find coincidence rates greater than 300 cps, as shown in Fig. 9.

To show that the photons are polarization-entangled, we measured coincidence rates as a function of the two polarizer orientations. The polarization correlations were strong enough to demonstrate a violation of a Bell inequality. We used the Clauser, Horne, Shimony, and Holt version of the Bell inequality $|S| \leqslant 2$ where S is a measure of the polarization correlation involving 16 coincidence measurements.[21] As described in the accompanying paper,[22] we found $S = 2.307 \pm 0.035$, a clear violation. The total acquisition time in this experiment was 240 s, and a fit to the coincidence data indicates more than 100 polarization-entangled photons per second. These data were taken with the irises fully opened.

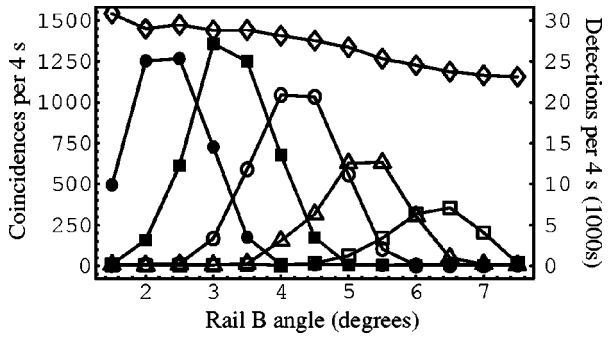

Fig. 9. Coincidence and singles detection rates as a function of detector positions. Closed circles, closed squares, open circles, open triangles and open squares show coincidence rates for $\theta_A = 2°$, 3°, 4°, 5°, and 6°, respectively, on left scale. Diamonds show channel B detection rate on right scale.

Closing down the irises will reduce the count rate, but may improve the purity of the detected entangled state.

VI. MISCELLANEOUS

A darkened room is necessary for the experiment, but complete darkness is neither necessary nor desirable. In our setup, black velvet curtains surrounding the work area block out sunlight and room lights. We found that a dimmed but visible computer monitor adjacent to the optical table gave negligible background coincidence counts. We use green LEDs behind BG-18 colored glass filters to illuminate the table; this green light cannot pass the RG780 filters to reach the detectors.

ACKNOWLEDGMENTS

We thank Paul Kwiat for inspiration and helpful discussions. This work was supported by Reed College and Grant No. DUE-0088605 from the National Science Foundation.

APPENDIX: SUPPLIERS AND EQUIPMENT NOTES

Below we list components of the apparatus that are unique or difficult to find, as well as suppliers for these components. These are also the most costly parts of the apparatus. Remaining components not described below include standard optical hardware such as mirror mounts, electronics to build the coincidence detector, and a means to record the detection rates.

Edmund Industrial Optics
101 East Gloucester Pike
Barrington, NJ 08007-1380
(800) 363-1992
http://www.edmundoptics.com

25.4-mm-diam unmounted linear glass polarizing filter. 2 in.×2 in. Polaroid near-IR linear polarizing film, (can be cut to make 1 in.×1 in. polarizers). 1-in.-diam RG-780 colored glass long pass filters (two). 1-in.-diam BG-12 blue-violet colored glass bandpass filter. 1-in.-diam BG-18 blue-green colored glass bandpass filter. Total cost: $255.

ILX Lightwave
P.O. Box 6310
Bozeman, MT
(800) 459-9459
http://www.ilxlightwave.com

LDX-3412 Precision Current Source. Cost: $846.

This model was chosen both for its precision and its compliance voltage. Most diode laser drivers cannot supply the 5-V operating voltage of the indium gallium nitride laser.

MTI Corporation
5327 Jacuzzi St. Bldg. 3H
Richmond, CA 94804
(510) 525-3070
http://www.mticrystal.com

SO*10 *x*-cut 5 mm×5 mm×0.5 mm quartz substrate, optically polished on both sides. Cost: $12. We glued this piece of quartz to a metal support to mount in an optic holder.

Nichia Corporation
Tokyo Technical Center
13F Tamachi Center Building, 34-7, Shiba 5-Chome
Minato-Ku, Tokyo 108-0014
Japan
http://www.nichia.co.jp

NLHV500C: 5-mW nominal wavelength 405-nm InGaN laser diode, 1000-h version. Cost: $1000. We tested two diodes, one with a wavelength of 400 nm, the other 406 nm, with very similar results. As InGaN laser diodes are a very young technology, it is reasonable to expect improvements in cost and lifetime in the near future.

Perkin–Elmer Optoelectronics
22001 Dumberry Road
Vaudreuil, Quebec J7V 8P7
Canada
(450)-424-3300
http://opto.perkinelmer.com

SPCM-AQR-13 Silicon APD Based Single Photon Counting Modules (two). Total cost: $7200. The -13 suffix describes the dark count rate. This has very little effect upon the coincidence count rate in the experiment, and any suffix model can be used. Note that the lead time for these detectors can be several months. Detectors require a +5-V power supply, not included.

Thorlabs, Inc.
435 Route 206
P.O. Box 366
Newton, NJ 07860
(973) 579-7227
http://www.thorlabs.com

C230TM-A: 0.55 NA aspheric lens, AR coated 350–600 nm. Collimating tube for 5.6-mm laser diode and C230TM-A. S7060: Laser diode socket for 5.6-mm laser. VC1 V-Clamp SPW301: 3/8-in. Spanner wrench. SPW602: SM1 Series Spanner wrench.. CP02: 30-mm threaded cage plate (two). HPT1: 30-mm cage X–Y translator (two). ER4: Extension rod, 4-in. long (eight). SM1V10: 1-in. adjustable focus tube for 1 in. optics (four). SM1V05: 1/2-in. adjustable focus tube for 1-in. optics (two). SM1T2: SM1 coupler, external threads (two). RSP1: Rotation stage for 1-in. optics (three). Total cost: $1040.

U-oplaz Technologies
21828 Lassen St., #D
Chatsworth, CA 91311
(818) 678-1999
http://www.u-oplaz.com

Two identical β-barium borate (BBO) crystals, 5 mm$\times$5 mm$\times$0.1 mm with a crystal cut of 29°, protective ''P-coating.'' Crystals custom-mounted face-to-face with one crystal rotated by 90° in a standard mount. Cost: $1400.

[a]Electronic mail: morgan.mitchell@reed.edu

[1]A. Einstein, B. Podolsky, and N. Rosen, ''Can quantum-mechanical description of physical reality be considered complete?'' Phys. Rev. **47**, 777–780 (1935).
[2]J. S. Bell, ''On the Einstein–Podolski–Rosen Paradox,'' Physics (Long Island City, N.Y.) **1**, 195–200 (1964). This article is reprinted in Ref. 3.
[3]A. K. Ekert, ''Quantum cryptography based on Bell's theorem,'' Phys. Rev. Lett. **67** (6), 661–663 (1991).
[4]D. S. Naik, C. G. Peterson, A. G. Whie, A. J. Berglund, and P. G. Kwiat, ''Entangled state quantum cryptography: Eavesdropping on the Ekert protocol,'' Phys. Rev. Lett. **84** (20), 4733–4736 (2000).
[5]T. Jennewein, C. Simon, G. Wells, H. Weinfurter, and A. Zeilinger, ''Quantum cryptography with entangled photons,'' Phys. Rev. Lett. **84** (20), 4729–4732 (2000).
[6]C. H. Bennett and S. J. Wiesner, ''Communication via one-particle and 2-particle operators on Einstein-Podolsky-Rosen states,'' Phys. Rev. Lett. **69** (20), 2881–2884 (1992).
[7]K. Mattle, H. Weinfurter, P. G. Kwiat, and A. Zeilinger, ''Dense coding in experimental quantum communication,'' Phys. Rev. Lett. **76** (25), 4656–4659 (1996).
[8]C. H. Bennett, G. Brassard, C. Crepeau, A. Jozsa, A. Peres, and W. K. Wootters, ''Teleporting an unknown quantum state via dual classical and Einstein-Podolsky-Rosen channels,'' Phys. Rev. Lett. **70** (13), 1895–1899 (1993).
[9]D. Bouwmeester, J.-W. Pan, K. Mattle, M. Eibl, H. Weinfurer, and A. Zeilinger, ''Experimental quantum teleportation,'' Nature (London) **390** (6660), 575–579 (1997).
[10]R. P. Feynman, ''Simulating physics with computers,'' Int. J. Theor. Phys. **21** (6-7), 467–488 (1982).
[11]D. Deutsch and R. Jozsa, ''Rapid solution of problems by quantum computation,'' Proc. R. Soc. London, Ser. A **439** (1907), 553–558 (1992).
[12]P. W. Shor, ''Polynomial-time algorithms for prime factorization and discrete logarithms on a quantum computer,'' SIAM J. Comput. **26** (5), 1484–1509 (1997).
[13]M. A. Nielsen and I. L. Chuang, *Quantum Computation and Quantum Information* (Cambridge U. P., Cambridge, 2000).
[14]P. G. Kwiat, K. Mattle, H. Weinfurter, A. Zeilinger, A. V. Sergienko, and Y. H. Shih, ''New high-intensity source of polarization-entangled photon pairs,'' Phys. Rev. Lett. **75** (24), 4337–4341 (1995).
[15]P. G. Kwiat, E. Waks, A. G. White, I. Appelbaum, and P. H. Eberhard, ''Ultrabright source of polarization-entangled photons,'' Phys. Rev. A **60** (2), R773–R776 (1999).
[16]C. K. Hong and L. Mandel, ''Theory of parametric frequency down conversion of light,'' Phys. Rev. A **31** (4), 2409–2418 (1985).
[17]P. Hariharan and B. C. Sanders, ''Quantum phenomena in optical interferometry,'' Prog. Opt. **36**, 49–128 (1996).
[18]R. W. Boyd, *Nonlinear Optics* (Academic, Boston, MA, 1992).
[19]Perkin-Elmer Optoelectronics, SPCM-AQR Single-Photon Counting Module Data Sheet.
[20]M. Ghioni, S. Cova, F. Zappa, and C. Samori, ''Compact active quenching circuit for fast photon counting with avalanche photodiodes,'' Rev. Sci. Instrum. **67** (10), 3440–3448 (1996).
[21]J. F. Clauser, M. A. Horne, A. Shimony, and R. A. Holt, ''Proposed experiment to test local hidden-variable theories,'' Phys. Rev. Lett. **23** (15), 880–884 (1969).
[22]D. Dehlinger and M. W. Mitchell, ''Entangled photons, nonlocality, and Bell inequalities in the undergraduate laboratory,'' Am. J. Phys. **70**, 903 (2002).